10363 Session 2022
B2 – Overhead lines
PS 2 / Last techniques in asset management, capacity enhancement, refurbishment

Application of a Fibre Bragg Grating-based sensing system for icing detection and structural health monitoring of Transmission Lines in Russia

Andrey VANYAKIN*
«Souztechenergo», JSC
Russian Federation
a.vanyakin@opten.ru

Andrey LIKHOBABIN
«Souztechenergo», JSC
Russian Federation
a.likhobabin@opten.ru

SUMMARY

In some regions of Russia, early detection of High-voltage overhead lines atmospheric icing is an important business process for the Transmission Grid. AC or DC Joule-heating de-icing are the main measure to avoid galloping and consequent damage. However, the maximum allowable de-icing time is limited by both technical and economic aspects. Hence, early and reliable detection is crucial.

A widely applied approach for detecting icing is the use of load cells to measure additional ice-induced weight. Conventional sensors contain electronic parts, batteries, and rely on wireless communication. Application practice has revealed some limitations of such technology, namely – limited data sampling rate, need for regular replacement of batteries, overall non-reliable operation in cold conditions and presence of strong EMF.

The authors have developed a solution aiming to satisfy the abovementioned need, but avoid present technical limitations by state of art. The main requirement for the solution – presence of Fiber-optic cable. The solution is based on utilizing load-cells containing Fiber-Bragg Gratings (FBG) strain and temperature sensors fiber-coupled (by means of the existing fiber-optic cable) with a substation-based measurement unit. Sag-Tension model is used to calculate ice load. As a result, the tower-based equipment becomes passive, can be operated at low temperatures, is immune to EMF and requires no maintenance.

This article aims to cover:

- description of the system's elements and their respective properties
- applied Sag-Tension model
- the process of installation and setup
- examples of field data, with and without icing
- the findings from the vibration spectra obtained with high sample rate measurements

KEYWORDS

Icing - Atmosphere, Overhead - Line, Sensing - Fibre-optic, Fibre - Bragg Grating, Monitoring - Structural

1. INTRODUCTION

Atmospheric icing is one of the major issues for the Russian Grid, specifically in the South, Volga, Urals regions, and the Far East. According to the design code [1], some regions are expected to have as much as 40 mm of dense glaze ice once per 25 years.

Since the late 2000s, most of the transmission lines subjected to heavy icing had been equipped with either AC or DC Joule-heating devices. At the same time, a wide application of icing detection sensors was introduced. The use of sensors would enable the Transmission operations staff with a possibility to make a weighted decision over de-icing initialization and monitor its effectiveness. Up to present day, hundreds of transmission line towers had been equipped with these sensors.

Figure 1 – Left - Russia's territory equivalent ice-thickness map, from [1]
Right – Transmission tower equiped with a conventional ice detection system including solar panels and utilizing wireless communication

A typical setup of a conventional sensing outpost (Figure 1, right) would consist of a piezoelectric load-cell installed in suspension insulator string, a battery, and a wireless communication system (mostly GSM). Depending on the manufacturer the power supply method is mostly the use of solar panels with seldom use of power harvesting. Some systems would also include an anemometer.

While still being an important tool in today's cold-time Transmission lines operation, the abovementioned technology had its limitations unveiled by a vast operation experience. The primary issue is the requirement to replace malfunctioned batteries each one-two seasons due to cold conditions. At times, sensors get outpowered for large periods during the cold-time season. The power supply factor does also limit the sampling and transmission rate of the sensor readings. Another issue is the use of GSM-communication to transfer data can be a location constraint for rural and hardly accessible areas.

As a response to these challenges, an attempt was made to create an industrial-ready icing-detection solution that the mentioned issues would be not applicable. Since a large number of Overhead lines are equipped or being designed with OPGW cables, a decision was made to target these lines to make use of fiber-optic sensing advantages while gaining side benefits from investment into the communication infrastructure

2. FIBER-OPTIC TENSION MEASUREMENT SYSTEM

2.1. Operation principle

Fiber Bragg Grating (FBG) is a short (typically 8-10 mm long) segment of single-mode fiber that reflects particular wavelength of light and transmits all others. This is achieved by creating a periodic variation of the refractive index of the fiber core, which acts as a wavelength-specific dielectric mirror. Sensing application of FBGs is possible due to a direct dependency between fiber elongation and the reflected wavelength (see Figure 2 – Left). A variety of FBG sensors are available and used widely for structural health monitoring. Fiber with an FBG is packaged into a carrier construction that protects the fiber and can be spot weld or epoxy glued to a surface.

The most widely used are strain and temperature sensors. Temperature sensors are composed in a way that the FBG does not perceive any mechanical strain. Strain sensors are affected by a combination of mechanical strain and thermal expansion of both the fiber and carrier. Mathematical compensation of thermal strain component, usually by means of using dedicated a temperature sensor, is essential to provide meaningful mechanical strain measurements.

Typical FBG strain sensor characteristics are:

- Strain range: ± 2 500 µm/m
- Sensitivity: better than 1 µm/m (mostly dependent on interrogator's capabilities)
- Operating temperature range: -40 °C to +120 °C
- Fatigue life, at least: 100 x 10^6 cycles of ± 2 000 µm/m

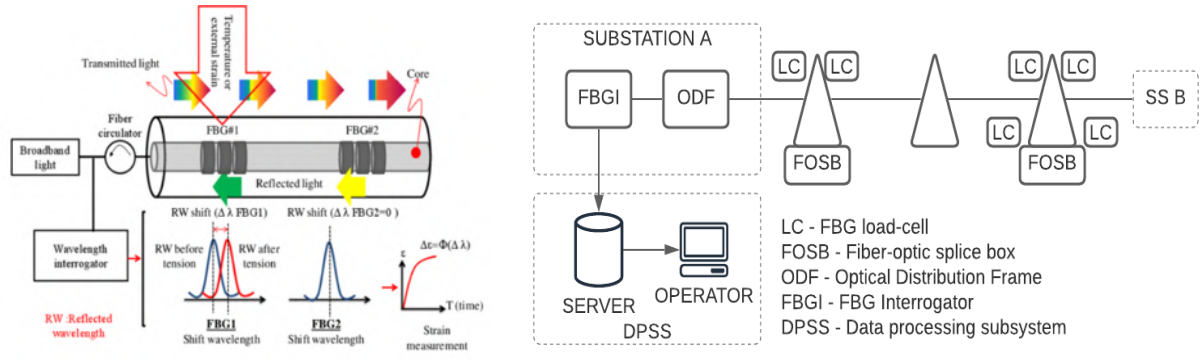

Figure 2 – Left – FBG sensing principle, from [2]
Right – Fiber-optic tension measurement system structure

The described system comprises (see Figure 2 - Right):

- FBG load-cells, installed into strain insulator strings, one tower can have multiple load-cells, multiple towers can be equipped; the tower must have a fiber-optic splice box
- One of the fibers from the existing fiber-optic cable
- Substation-based FBG interrogator unit, connected to one of the fibers by means of the optical distribution frame (ODF)
- Data acquisition, storage and presentation subsystem (server and software)

2.2. Load-cell

The load-cell (see Figure 3) combines functions of a transmission line fitting, tension and temperature sensor, fiber-optic splice box and hence had been designed and tested accordingly.

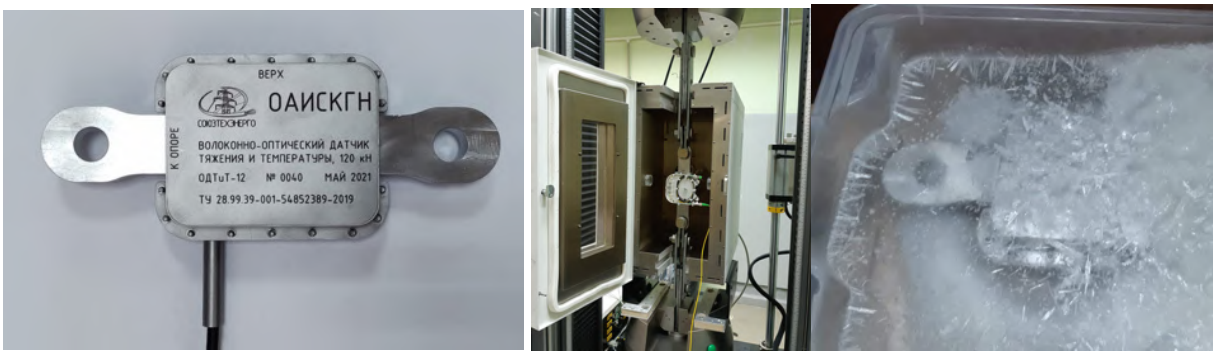

Figure 3 – Left to Right
FBG load-cell, testing on a tensile machine with a temperature chamber, freeze-thaw testing

A corrosion-resistant alloy is used to manufacture the load-bearing element. Elements are manufactured per rated tensile strength class, with respect to the mounting dimensions of standard fittings. The failure load tests are conducted in accordance with [3].

The internals of the sensor are covered with a corrosion-resistant enclosure, consisting of two parts, sealed with a UV-resistant silicone compound. Assembly technology had been tested to sustain 1 atm

(10 m) of water pressure for an hour and at least 10 cycles of freeze-thaw tests. Each assembled sensor is calibrated on a tensile testing machine. Load-cells are supplied on a drum with 80m meters of cable terminated with a compact splice box with connectors.

2.3. Sensing instrument

The main challenge of adapting FBG sensing to a practical overhead line application – is the measurement on long distances. Most structural health monitoring applications using FBGs comprise multiple sensors, but relatively short distances between the instrument and the sensors. For overhead lines the distances are tens of kilometers at the least.

The light has to travel to a remote tower and back keeping enough signal amplitude to be detected. The FBG interrogators operate in the SCL-band (1460 – 1625 nm), apart from the insertion loss from the light traveling long distance, it is the Rayleigh backscattering effect that does also cut the effective dynamic range.

Significant effort was made to define the balance between instrument accuracy, sampling rate and reach. Additional measures are taken on the sensor side to ensure minimal insertion loss. The achieved interrogator setup consists of a swept light source interrogator with a 10 Hz sampling rate. The instrument has confirmed reach of 65 km. For longer lines, reach can be doubled by placing a second instrument on peer substation.

The measurements absolute accuracy is not worse than 1 pm (roughly corresponds to 1 μm/m relative elongation or 1/30 °C) in wide temperature range. 100 and 160 nm wavelength ranges provide enough bandwidth to multiplex multiple sensors. Up to 16 fibers can be interrogated simultaneously.

2.4. Software and Sag-tension model

The load-cell's measurement is the tension calculated from FBG strain. In order to calculate ice load a reference Sag-Tension model with Experimental Plastic Elongation (EPE) [4] is created for each installed sensor. PLS-CADD software is used to create the initial model coefficients given the most accurate available information on the cable properties and line composition. Later, after installation and some operation period, the models are usually refined based on measured data.

The user-facing application (see Figure 3) is subscribed to live measurements stream. Operator can see current measurements (Tension, Temperature, Ice load in Equivalent Thickness, mm or Ice weight kg / 200m) on a dashboard and charts. An interactive map displays sensor's locations. Adjustable Ice load thresholds color code values based on threat level.

Based on the model, the system calculates and displays the expected tension range. Icing detection happens automatically based on several criteria.

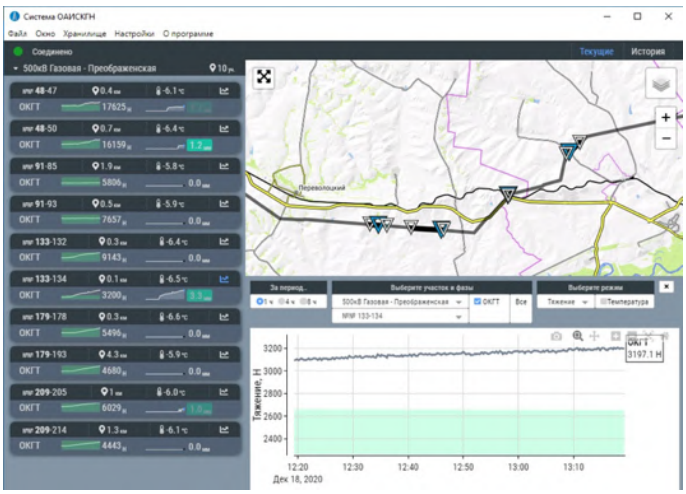

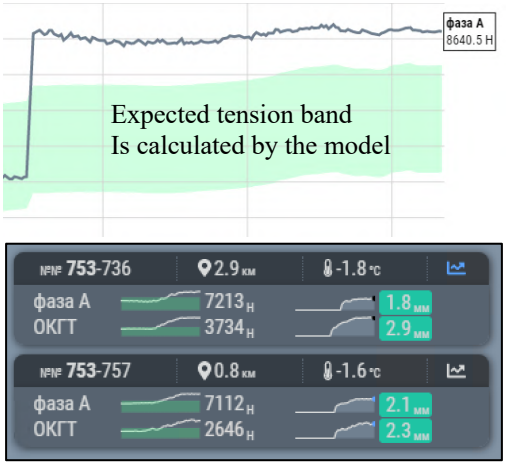

Dashboard with Tension and Ice load micro charts

Figure 3 – User-facing application

3. FIELD EXPERIENCE

3.1. Application record

At present time, the fiber-optic tension measurement system is installed on four overhead lines (see table I, Figure 4)

Table I – List of lines equipped with fiber-optic tension measurement system

№	Line voltage class and region	LCs* Qty	Year	Comments
1	330 kV, South, Caucasus foothills	5	2015	Pilot project. OPGW and Duplex ACSR Hawk
2	500 kV, South Urals	10	2019	OPGW
3	220 kV, Central Russia, Volga basin	8	2020	OPGW and ACSR Peacock
4	220 kV, Central Russia, Volga basin	8	2020	OPGW and ACSR Condor

* - load-cells

Figure 4 – FBG load-cells installed on Overhead Lines

3.2. Installation and setup

Mounting of the load-cell is performed using common line men techniques and tools. During the mounting, the sensor is connected to an on-site measurement instrument and reading are observed by supervising engineer. After the mounting and cable management is over, load-cell's fibers are spliced with the fiber leading to substation.

Once all load-cells are installed and fibers spliced. The data acquisition software is being setup. After that, the system does not require additional attendance.

3.3. Measurements examples and discussion

The proof of concept was obtained during the Pilot project started on 2015 on a 330 kV line and the prior year where a prototype was installed on a test span. During the first year of pilot, several mild ice accretion cases were observed. System's readings were compared to a conventional icing detection system used on that line and meteorological data. The results were found to have a very good correlation.

Figure 5 depicts Ice accretion cases as they can be seen in the System's application. Left-top picture shows a significant increase of tension, leading away from the "normal" band. Right-top corner – minor tension increase, wet snow accretion self-disappeared at noon due to solar radiation.

Second row of pictures demonstrate the effect of Joule-heating de-icing on Duplex Hawk conductor, on both tension and equivalent ice thickness plots.

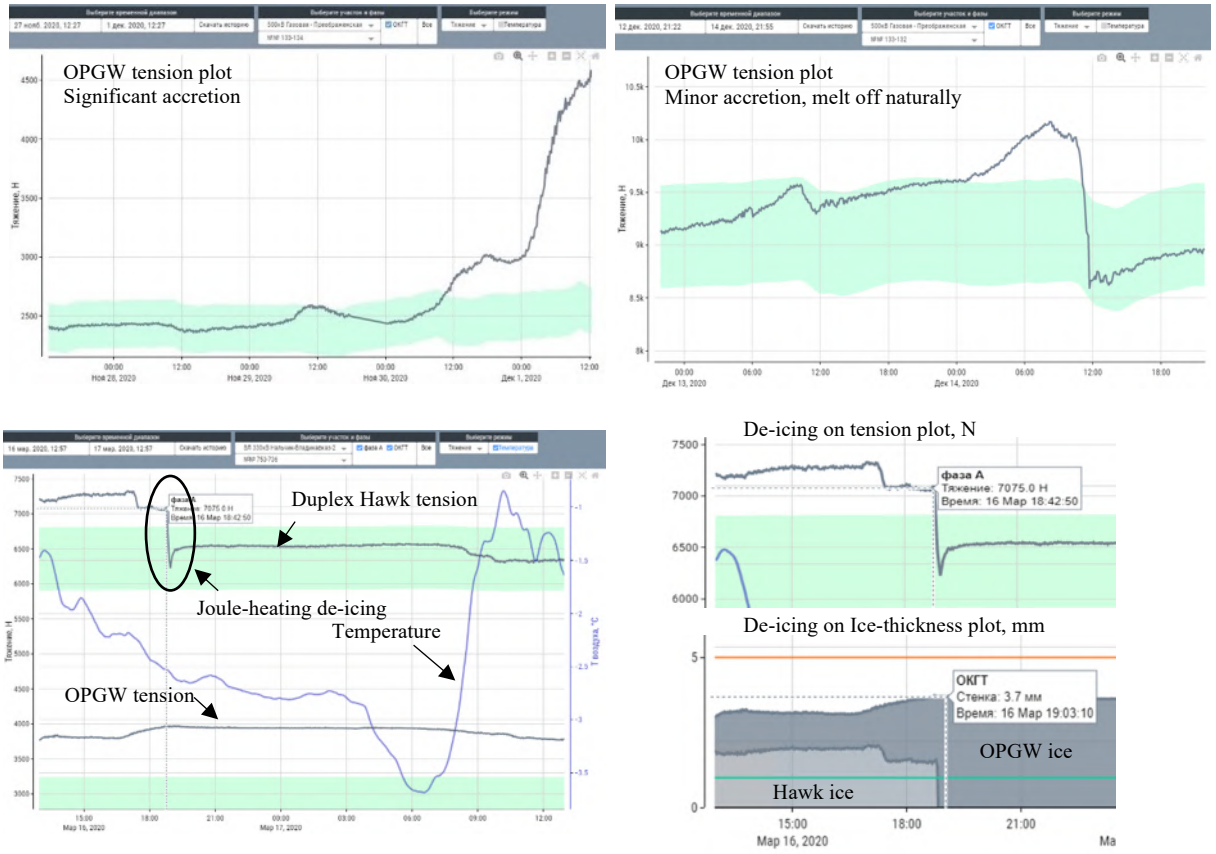

Figure 5 – Ice accretion events as seen in System's application

Figure 6 demonstrates distribution of ice load on a 11,1mm OPGW along 65 kms of line and five sensing outposts. Each tower is equipped with two load-cell for incoming and outbound sections. The icing event that took place on Jan 10th 2021 around the city of Orenburg. According to the meteorological data archive (as available at www.rp5.ru) conditions favoring rime-icing were observed, such as 90-100% RH and air temperature close to 0 °C. Ice-load values are presented in kgs / 200 m of cable.

Another typical icing mist event is demonstrated on Figure 7, for ACSR Peacock. As observed in Saratov Region on Jan 9th 2021 – 100% RH and air temperature falling to 0 °C.

Figure 8 represents tension as a function of temperature plots for 11,1mm OPGW and ACSR Peacock based on measurements archive. It can be noted, that icing can be clearly seen for both cable types.

ACSR Peacock data (right chart) is shown in two datasets – all measured data (in orange) and nightly only data (from 00:00 to 05:00, in blue). The effect of solar radiation and line current load can be seen when comparing the two datasets. The temperature used for the plot is measured inside the load-cells housing, however, the actual conductor's temperature is higher during daytime.

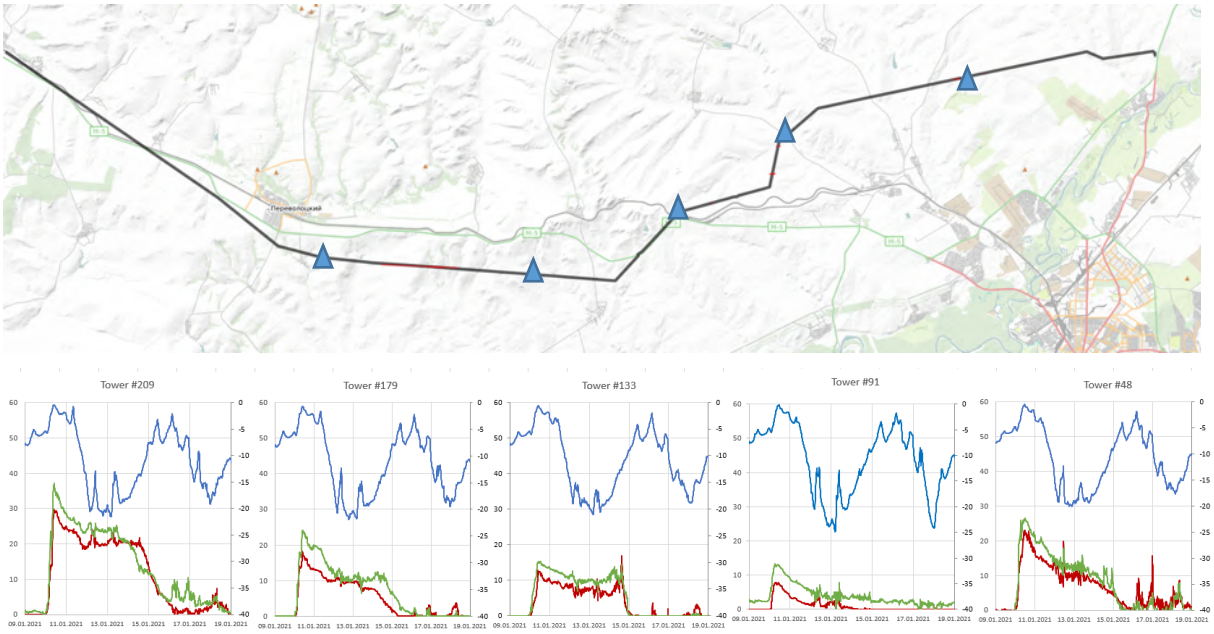

Figure 6 – Distribution of ice load on 11,1mm OPGW along 65km of line. Two sensors per tower.
Red and Green – ice load measured by the system (kg/200 m, left Y-axis)
Blue – temperature, °C, right Y-axis

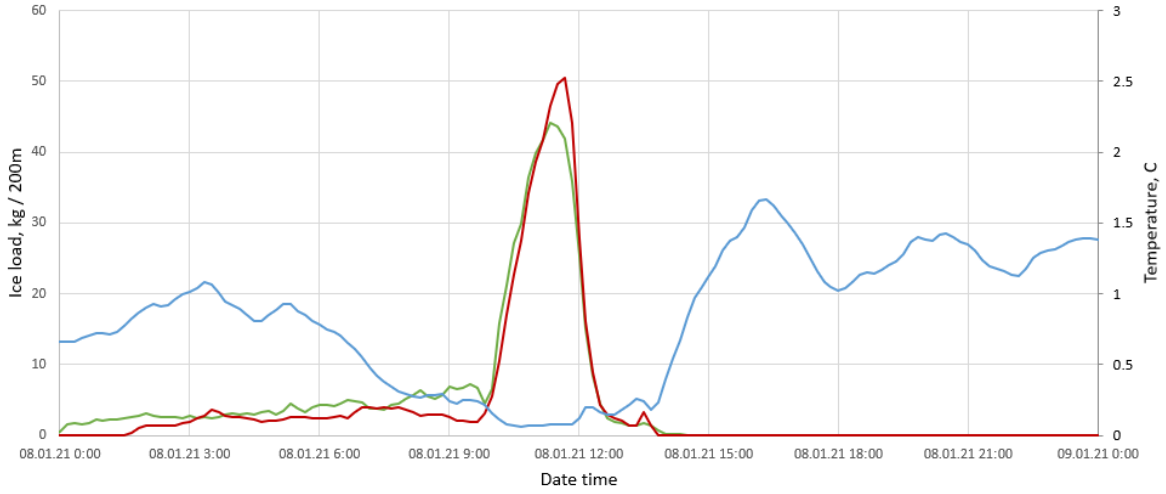

Figure 7 – Icing mist event. ACSR Peacock, two load-cells, ice load in kg/ 200 m

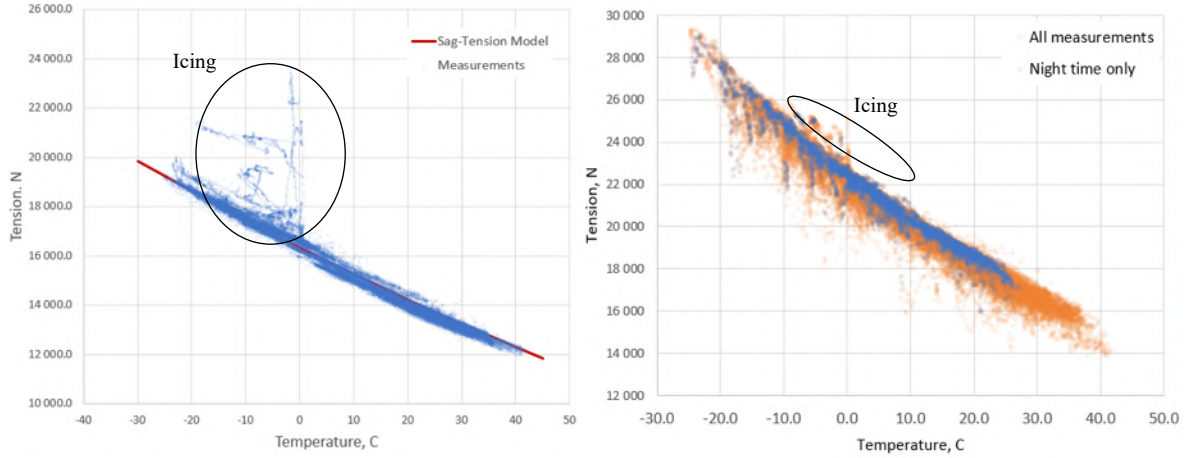

Figure 8 – Tension-Temperature plot of Left – 11,1mm OPGW; Right – ACSR Peacock

4. VIBRATRION SPECTRA ANALYSIS

4.1. Methodology

During the pilot installation on the 330kV line several measurement instrument setups were tested. One of the setups comprised an Amplified Spontaneous Emission (ASE) light source and high sampling rate detector. That instrument had inferior precision to swept-laser technology, but was capable of providing up to 5 kHz sampling rate.

The data, obtained during that period has led to another branch of research of the application of FBGs for exploring the behaviour of overhead lines,

The described instrument was used to measure tension fluctuations with a sample rate of 800 Hz for a period more than six months. In order to analyse the fluctuations in time-frequency domain, the Short-Time Fourier Transform (STFT) (see Fig. 9) was applied to 800 Hz time series. Best results were obtained with a window length of 20 seconds and Hamming window function.

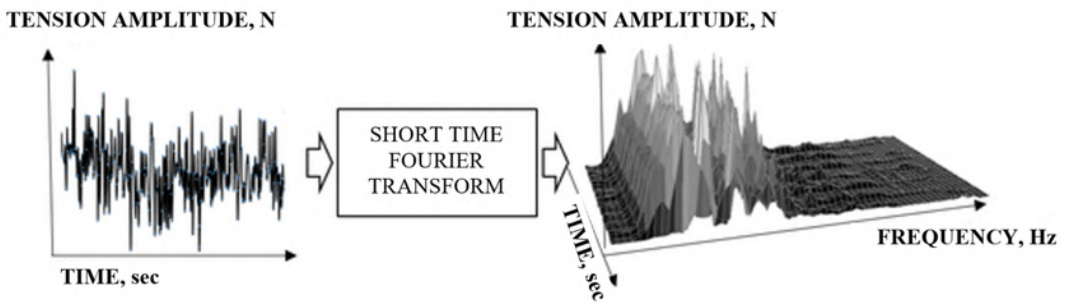

Figure 9 – Short-time Fourier Transform

The results of STFT transformation were then visualized as s Spectral Density Plot and analyzed. Several interesting phenomena were observed.

4.2. Conductor natural frequencies

The first finding was that the span natural frequencies of individual cables were clearly observable (see Figure 10 for OPGW and Duplex ACSR Hawk spectral density plot). The values of individual frequencies were found to be very close to theoretical values calculated with the simplified equation for conductor natural frequencies.

The Duplex ACSR Hawk natural frequencies were less distinguishable on the spectrogram. The assumption was made that the frequencies of individual conductors of the duplex interfere one with each other.

The conclusion was made, that the tension fluctuations registered by the FBG load-cell interrogated at a high sample rate can be a reliable source of information on the span's spectral footprint.

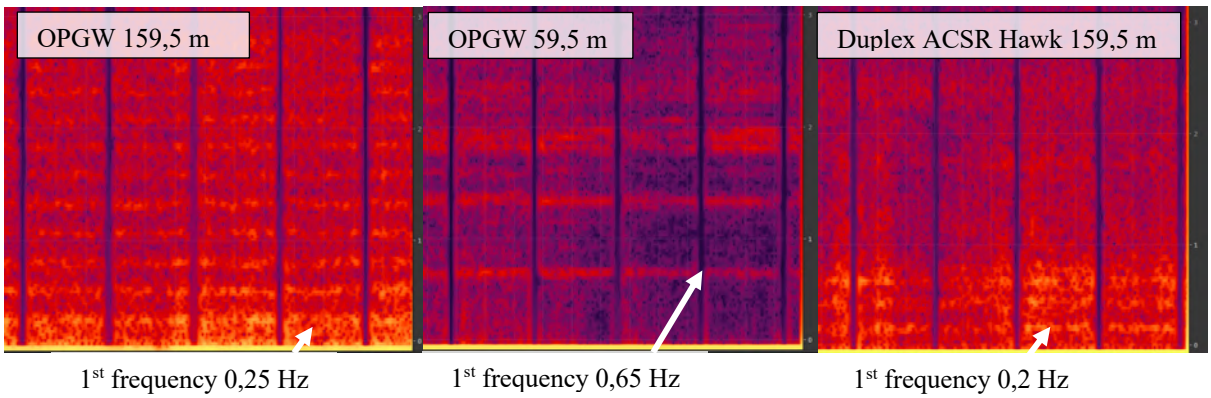

Figure 10 – Spectral Density Plot (X axis – Time, Y axis – Frequency, Color Brightness – Amplitude)

4.3. Wind-speed calculation and effects of environmental impact

It was also observed that the fluctuation energy (visualised as colour intensity on the plots) is changing over time. Figure 11 represents spectral density plot of OPGW tension fluctuations during a hail storm that took place around the city of Vladikavkaz on Jun 5th 2016. Strong winds and hail as large as 4-5 cm in diameter were reported that day.

The assumption was made that the fluctuation energy (visualised as colour intensity on the plots) and the highest visible frequency, are primarily dependent on the effective wind speed. Strouhal equation (1) was used to calculate theoretical effective wind speeds from the highest deducible natural frequencies (see markers at Fig. 11)

$$St = \frac{f \cdot d}{U} \qquad (1)$$

where, f – vortex shedding frequency,
d – diameter of the cylinder
U – flow velocity

And algorithm was created to calculate wind speed from the spectral density distribution. The algorithm did not take wind direction into account as it was unclear how to deduce wind direction from vibration spectra.

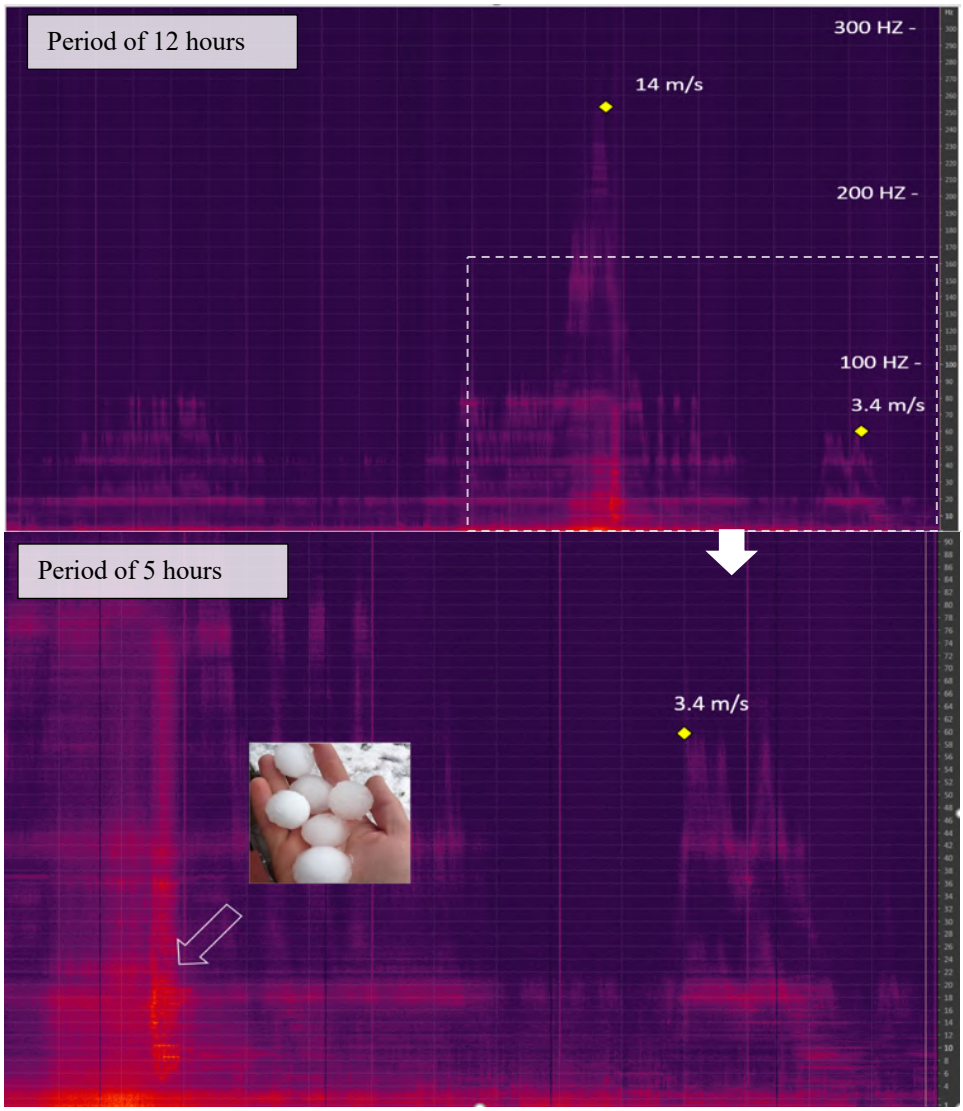

Figure 11 – Spectral Density Plot of OPGW during a hail storm
Markers – wind speeds calculated using the Strouhal equation

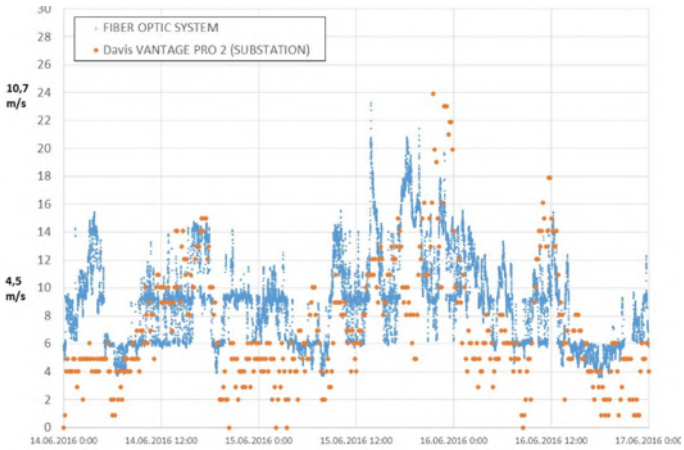

Figure 12 – Comparison between wind speed calculated with the alogrithm utilizing the Strouhal equation (blue) and measured by a conventional Anemometer. Distance to Anemometer location – 25 km

The nearest available anemometer was located in 25 km in substation premises. Given that both locations are situated on the same plane it was considered reasonable to compare the anemometer wind speed readings with the effective wind speed calculated from the spectra. Taking the distance into account, the results (see Fig. 12) represent reasonable correlation.

The provided results demonstrate that the high sampled data registered by the Fiber-optic tension measurement system can be used to assess effective wind speed and environmental effects on the conductor. H

4.4. Electric field and conductor icing

Another phenomena that was observed on Duplex ACSR Hawk – presence of a set of vibration components with frequency values multiple of the grid's frequency (i.e., 50 Hz, 100 Hz. 150 Hz etc.). With the most "energized" component having frequency close to 100 Hz.

It was observed that while the frequency value of the component is not changing over time, the amplitude could vary significantly from noise level to 15-16 times the noise level.

A correlation has been revealed between the amplitude of 100 Hz component and precipitation. Left part of Figure 13 demonstrates change in 100 Hz signal to noise ratio (noise level measured around the 100 Hz level) over a month.

It was registered that during a confirmed ice accretion event (3.2 mm of equivalent glaze ice thickness) the S/N ratio levels were as high as 16, while being in 3-4 range most of the time. It was also apparent that the phenomena only took place in presence of electric field. A confirmed wet snow accretion event was observed between March 14th to 18th but did not cause S/N increase because the line was de-energized.

A more detailed investigation of March 20th ice accretion reveals (see Figure 13, right) that the 100 Hz S/N ratio is changing whereas the tension, caused by ice load is relatively stable. It is noted that a surge of S/N ratio is observed during the ice meltdown process.

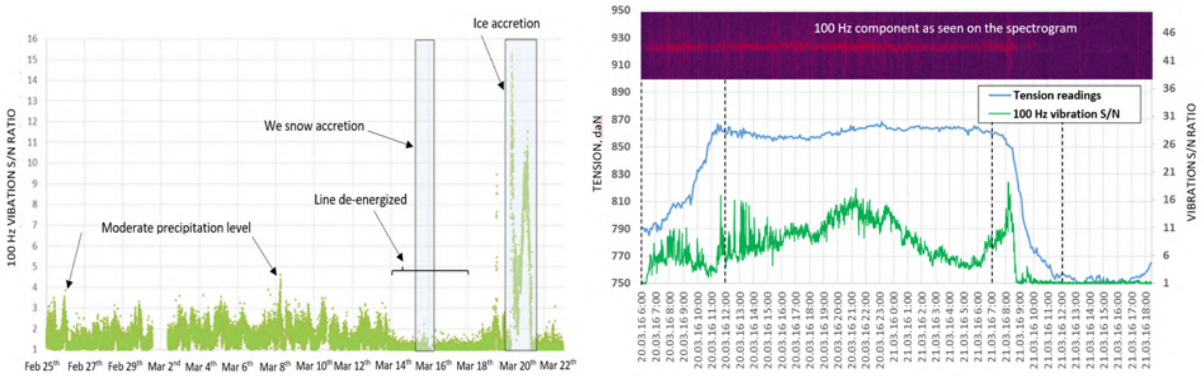

Figure 13 – 100 Hz component S/N ratio
Left – period of one month, Right – details on Ice acretion case on March 20th

A possible explanation to the described phenomena was found in [5]. One of the observations made by the authors is that the water droplets on the conductor surface have an interaction with the line's electric AC field that results in droplet vibration with frequency twice the field's frequency. Thus, An AC 50 Hz line will induce 100 Hz droplet oscillations (see Figure 14). The droplet vibration intensity is found to be a function of electric surface gradient and the amount of droplets.

It appears that ice and snow acretion affects both items causing 100 Hz to rise – surface gradient is disturbed due to cross-section form change and conductor surface is covered with liquid.

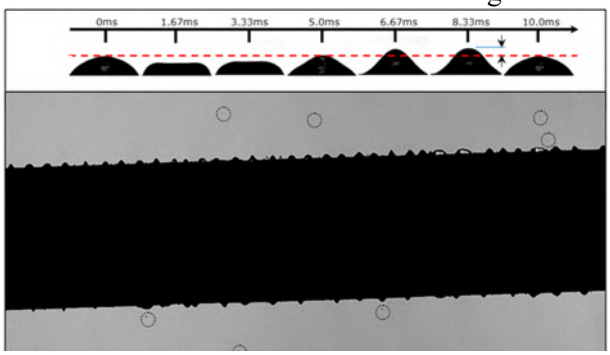

Figure 14 – Droplets oscilating on conductor surface, from [5]

Even though the correlation of ice load and 100 Hz S/N ratio seems apparent, the measure of ice load provided is rather indicative and relative than qualitative. For each installation the S/N ratio values have to be calibrated versus the ice load measured by the load-cell. It is also important to note, that the base electric surface gradient level can change over time due to conductor surface pollution or broken wires. The presented data was obtained on a Duplex ACSR Hawk conductor on a 330 kV line, additional experiments on lower voltage lines are required to validate the results.

5. CONCLUSION

This paper describes how the advantages of a fiber-optic sensing technology were carefully adapted to fit a particular overhead lines application, resulting in creation of an industrial-grade system. Measurement data during both icing and de-icing was presented and discussed.

In addition, the prospect of using FBG sensors to research vibration spectra of overhead line conductors on energized lines was demonstrated.

The work on this system started in early 2014. At present moment 4 overhead lines are equipped with 35 FBG load-cells. No load-cell failures were registered. The data acquisition is being performed without interruptions with a 10 Hz sampling rate. The sensing outposts do not require maintenance.

The application of the proposed system is only possible for overhead lines equipped with fiber-optic cables. Another constraint is that the sensors can be only places on towers with splice boxes. However, based on author's experience, finding a proper location to place the sensing outpost has never been a challenge as the distance between splice boxes is usually between 4-6 km.

The creators of the system were mainly focused on the icing detection application. However, the presented system is not limited to icing detection scope and can be considered to be a conductor structural health monitoring system. Additional possible use cases, including application for dynamic-line rating are to be researched in the future.

BIBLIOGRAPHY

[1] Ministry of Construction of Russia “Russia’s Structural Design Code. Loads and actions” (SP.20.13330.2016, 2017)

[2] Malekzadeh, Masoud & Gul, Mustafa & Kwon, Il-Bum & Catbas, Necati. “An integrated approach for structural health monitoring using an in-house built fiber optic system and non-parametric data analysis.” (Smart Structures and Systems. 14. 917-942. 10.12989/sss.2014.14.5.917, 2014)

[3] IEC, TC 11 – Overhead lines “Overhead lines – Requirements and tests for fittings” (IEC 61284, p. 35)

[4] CIGRE Task Force B2.12.3 “Sag-Tension Calculation Methods for Overhead Lines” (TB 324, , p. 61, 2016)

[5] Qi Li, S.M. Rowland “Wet conductor surfaces and the onset of corona discharges” (IEEE Conference on Electrical Insulation and Dielectric Phenomena, pp. 245-248, 2015)